Electrochemical and Solid-State Letters, **8** (11) B65-B68 (2005)
1099-0062/2005/8(11)/B65/4/$7.00 © The Electrochemical Society, Inc.

The Effect of Cu Content on Chromate Conversion Coating Formation of Compositional Analogs of the η Phase $Mg(Zn,xCu)_2$

Yuhchae Yoon* and R. G. Buchheit,z**

Fontana Corrosion Center, Department of Materials Science and Engineering, The Ohio State University, Columbus, Ohio 43210, USA

Thin film compositional analogs of the intermetallic compound η, $Mg(Zn,xCu)_2$ ($0 \leqslant x \leqslant 35$ atom %), found in high strength Al-Zn-Mg-Cu alloys were fabricated using a flash evaporation technique for characterization of electrochemical behavior and for chromate conversion coating formation experiments. In potentiodynamic polarization measurements in deaerated 0.1 M NaCl, the open-circuit and breakdown potentials increased and dissolution rates decreased with increasing Cu content of the analogs. When the analogs were chromate conversion coated from a ferricyanide-accelerated coating bath, Raman spectra showed that coating thicknesses decreased with increasing Cu content. Other coating formation experiments showed that ferricyanide additions to the coating bath acted as a coating formation accelerator for $MgZn_2$. However, coating formation was so strongly inhibited for the Cu-bearing analogs, that the effect of ferricyanide on coating formation was indiscernible.
 [DOI: 10.1149/1.2073629]

Manuscript submitted December 9, 2004; revised manuscript received June 29, 2005. Available electronically September 22, 2005.

$MgZn_2$ is an important strengthening phase in Al-Zn-Mg-Cu alloys. This phase forms by nucleation and growth processes during artificial aging of a supersaturated solid solution (SSSS) on grain boundaries and within grains resulting in a uniform, high number density dispersion of fine precipitates. The precipitation sequence is[1-11]

$$\text{SSSS} \rightarrow \text{GP} \rightarrow \eta' \rightarrow \eta(MgZn_2) \qquad [1]$$

where GP denotes Guinier-Preston zones. This precipitation process contributes greatly to alloy strengthening. Larger precipitates form on grain boundaries than in the matrix and attempts to measure grain boundary precipitate chemistry show that the phase contains Cu and perhaps Al as aging progresses from peak to overaged tempers. While precise chemistries have been difficult to obtain, the solubility for Cu and Al is so extensive, that $MgZn_2$ and AlCuMg are isostructural.[2,12]

It is observed that localized corrosion susceptibility of Al-Zn-Mg-Cu alloys changes significantly from peakaged to overaged tempers. The overaged temper exhibits lower pitting potentials, but is less susceptible to intergranular corrosion. Distinctive differences in localized corrosion morphologies mainly related to the occurrence of intergranular corrosion have also been noted.[13-16]

The electrochemistry of compositional analogs of compounds ranging in chemistry from $MgZn_2$ to near AlCuMg has been characterized using polarization techniques.[17] Results show that while the phase remains electrochemically active with respect to polarization behavior of Al-Zn-Mg-Cu alloys of commercial composition, increasing Cu content in the phase increases the corrosion and pitting potentials and decreases the passive current density. These effects are most pronounced when the Cu content exceeds 20 atom %. Additions of Al up to 10 atom % have a comparatively minor effect on the polarization response. While the change in intergranular corrosion susceptibility of Al-Zn-Mg-Cu alloys and ennoblement of η-phase dissolution kinetics with increase aging has been noted, there is no broad agreement on a causal relationship.[13-15,18]

Alloy temper also affects the formation and protectiveness of chromate conversion coatings (CCCs) on Al-Zn-Mg-Cu alloys. For alloy 7475, conversion coatings were slightly more protective when applied to overaged (T7) material than to peakaged (T6) material.[19]

The apparent link between the η-phase chemistry, η-phase electrochemical behavior, and alloy corrosion behavior suggests the possibility of a relation between the dependence of CCC formation and breakdown behavior, and η-phase chemistry.

In this study, thin-film compositional analogs of η-phase were fabricated using a flash evaporation method. The thickness of 3-min CCCs on η-phase with different Cu contents was determined by Raman spectroscopy. Additionally, the effect of ferricyanide on the formation of chromate conversion coating on Cu-bearing η-phase was examined. Results confirm previously reported effects of Cu on electrochemical behavior of η, and clarify the nature of the interaction of $Fe(CN)_6^{3-}$ as Cu content in η increases.

Experimental

Thin-film analogs of $\eta(Mg(Zn, xCu)_2)$ were produced using a flash evaporation technique following the procedure of Ramgopal et al. using alloy powder feedstock produced by grinding cast ingots.[17] Samples with four different Cu contents ranging from 0 to 35 atom % were prepared. The operating pressure of the flash evaporation chamber was kept below 2×10^{-7} Torr in order to minimize oxygen contamination.[17] The thin films were deposited on Si wafers for electrochemical testing. The nominal thickness of the analog films was up to 2 μm for Si wafer substrates. After deposition, the compositions of thin-film analogs were checked using energy dispersive spectroscopy (EDS) and had compositions corresponding closely to the composition of the powder feedstock. Ramgopal characterized the thin films using Auger electron spectroscopy (AES) depth profiles and atomic force microscopy (AFM) topography image and Volta potential map.[17] These thin films were reasonably homogeneous. The samples prepared had the following compositions expressed on an atomic percentage basis and are referred to using their approximate stoichiometric ratios: 33Mg-67Zn($MgZn_2$), 33Mg-50Zn-17Cu($Mg_3Zn_5Cu_2$), 33Mg-42Zn-25Cu($Mg_3Zn_4Cu_3$), and 33Mg-32Zn-35Zn (MgZnCu). The variation in composition was less than 1 atom % for each element in each sample. The extent to which these specific phases are present in Al-Zn-Mg-Cu alloys is unknown, however important aspects of the trends in the electrochemical behavior and formation of conversion coatings as a function of Cu content on the η-phase should be reflected in experiments conducted with these samples.

Anodic polarization experiments were carried out in a flat cell using a three-electrode configuration comprising a Pt counter electrode, a saturated calomel reference electrode, and the thin-film analog working electrode. Scans were initiated below the steady-state corrosion potential and were continued past the apparent breakdown or pitting potential. All scans were carried out in deaerated 0.1 M NaCl solution at a scan rate of 0.2 mV/s. The electrolyte was deaer-

* Electrochemical Society Student Member.
** Electrochemical Society Active Member.
z E-mail: buchheit.8@osu.edu

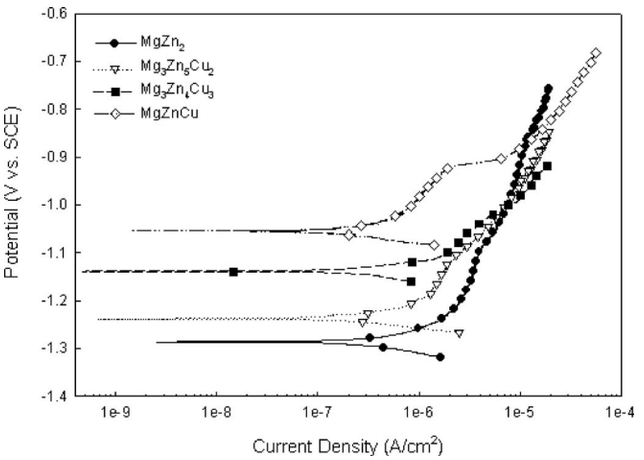

Figure 1. Polarization curves of $MgZn_2$, $Mg_3Zn_5Cu_2$, $Mg_3Zn_4Cu_3$, and MgZnCu at a scan rate of 0.2 mV/s in deaerated 0.1 M NaCl.

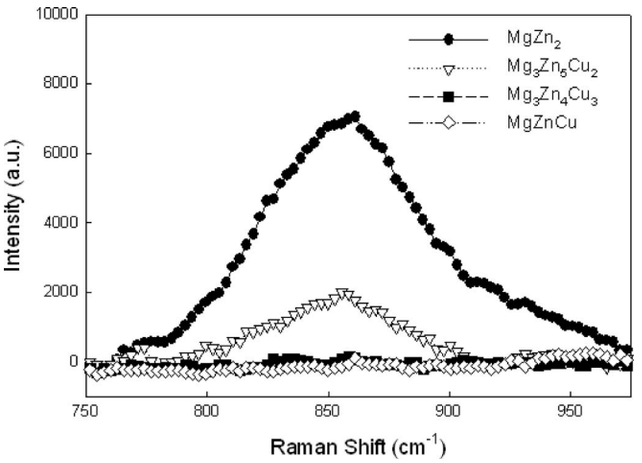

Figure 2. Raman spectra of 3-min CCCs on $MgZn_2$, $Mg_3Zn_5Cu_2$, $Mg_3Zn_4Cu_3$, and MgZnCu in Alodine 1200S bath.

ated by bubbling argon through the solution for at least 1 day before immersing the specimen. The solution was sparged throughout the experiment.

Chromate conversion coatings were applied to thin-film analogs by simple immersion of the samples at their respective open-circuit potentials. The coating bath was stirred during the experiment. Coatings were applied using a ferricyanide-accelerated Alodine 1200S conversion coating bath formulation. The bath chemistry ranges given in manufacturer's specifications (Henkel Surface Finishing Technologies, North America, Madison Heights, MI) are 3.95–4.74 g/L CrO_3, 0.79–2.37 g/L $K_3Fe(CN)_6$, 0.79–2.37 g/L KBF_4, 0.08–0.79 g/L NaF, and 0.08–0.79 g/L K_2ZrF_6.[20] For certain experiments, ferricyanide-free conversion coatings were applied from conversion coating baths prepared in-house. The chemistry for these baths was 5.4 g/L CrO_3, 0.9 g/L $K_3Fe(CN)_6$, and 0.9 g/L NaF. In this case, other supplemental ingredients present in Alodine 1200S were deliberately withheld. The CrO_3, $K_3Fe(CN)_6$, and NaF concentrations in both types of baths were somewhat different from one another, but were well within ranges used for chromate coating formulations. These chemistry differences were not expected to result in different coating formation characteristics. To understand the effect of ferricyanide of the bath in the coating formation on η-phase, an in-house conversion coating bath with ferricyanide withheld was synthesized. The chemistry for these baths was 5.4 g/L CrO_3 and 0.9 g/L NaF.

The thickness of CCCs formed on the compositional analogs was estimated from the peak intensity of the 860 cm^{-1} Raman scattering band, which is due to scattering by Cr^{6+}-O-Cr^{3+} bonds in the CCC structure.[21,22] Samples were interrogated using a 514.5 nm laser, a 180° backscattered sampling geometry, and a laser spot size of about 50 μm diameter. The peak height at 860 cm^{-1} was analyzed after baseline correction. Peak intensity values used in this estimate were averages taken from four separate scans at three different locations on the sample surface (12 total scans). Scan-to-scan variations in peak intensity on a given sample were less than 1%.

Results and Discussion

Effect of Cu on the anodic polarization behavior of the compositional analogs.— Figure 1 shows anodic polarization curves for the compositional analogs in deaerated 0.l M NaCl. The polarization curves for $MgZn_2$ and $Mg_3Zn_5Cu_2$ are similar with corrosion potentials between −1240 and −1300 mV, and passive regions where the dissolution rates are several μA/cm^2. Both curves exhibit poorly defined breakdown potentials at about −1100 mV, above which the dissolution rate gradually increases from tens to hundreds of μA/cm^2. This breakdown has been noted previously and has been attributed to the onset of Zn oxidation from the phase.[17] In these experiments, breakdown occurs at a potential that is about 100 mV more positive than the reversible potential of Zn, which was estimated to be −1180 mV assuming a Zn^{2+} concentration of 10^{-6} M.

The polarization response of the MgZnCu analog exhibited significantly increased corrosion and breakdown potentials and a reduced passive current density compared to the other two analogs. The breakdown potential is very clearly defined and occurs well positive of the expected reversible potential for Zn. The polarization curve of $Mg_3Zn_4Cu_3$ analog is showing intermediate corrosion and breakdown potentials. Whether breakdown is associated with the onset of Zn oxidation or the breakdown of a protective Cu-rich surface film that forms during polarization is not obvious.

These data illustrate the increase in passivity and nobility associated with an increase of Cu content in η. However, even at very high Cu concentrations η is still an anodic phase in Al-Zn-Mg-Cu alloys where the free corrosion potential ranges from −700 to −750 mV in aerated dilute chloride solutions.

Effect of Cu content in compositional analogs on CCC formation.— CCC formation on Al-Cu-Mg intermetallic compounds is increasingly inhibited as the Cu content of the phase increases.[23] The same appears to be true for η as its Cu concentration increases. Figure 2 shows the 860 cm^{-1} Raman band for CCCs formed by a 3-min immersion in the Alodine 1200S bath. The band is intense for $MgZn_2$ suggesting robust CCC formation. However as Cu content increases, band intensity diminishes markedly. A weak band is observed for $Mg_3Zn_5Cu_2$, and evidence of CCC formation on $Mg_3Zn_4Cu_3$ and MgZnCu is completely absent. Figure 3 also shows the Raman spectra in the vicinity of the 860 cm^{-1} peak for CCCs formed by 3-min immersion in a conversion coating bath consisting of CrO_3 + $K_3Fe(CN)_6$ + NaF but lacking other minor ingredients noted earlier. The CCC formation on $MgZn_2$ is observed clearly while formation on $Mg_3Zn_5Cu_2$, $Mg_3Zn_4Cu_3$, and MgZnCu is absent.

In another class of electrochemically active, Cu-bearing intermetallic compounds, Al-Cu-Mg, CCC formation was suppressed by surface adsorption of ferricyanide on Cu sites.[23] This adsorbed layer appeared to passivate the compounds suppressing normal CCC formation, but this layer itself did not appear to confer the level of corrosion protection provided by CCCs.

Effect of ferricyanide in CCC formation on η.— The presence of ferricyanide in a CCC bath had a significant effect on CCC formation on the compositional analog of η. Figure 4 shows Raman spectra in the vicinity of the 860 cm^{-1} peak. There is evidence of strong CCC formation when coating is carried out in a ferricyanide

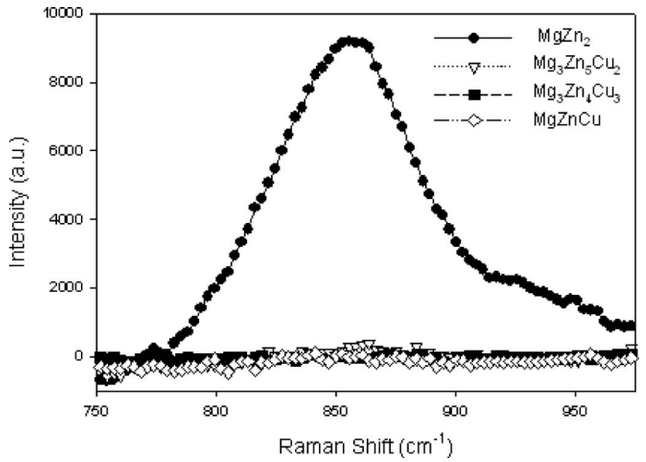

Figure 3. Raman spectra of 3-min CCCs on $MgZn_2$, $Mg_3Zn_5Cu_2$, $Mg_3Zn_4Cu_3$, and MgZnCu coated in a (Cr + F + Fe) bath consisting of CrO_3 + $K_3Fe(CN)_6$ + NaF.

containing bath. However, when coating is carried out in a bath where ferricyanide is withheld, coating formation is much weaker. This result shows that ferricyanide is an accelerator of CCC formation on η.

Figure 4 also shows Raman spectra collected from $Mg_3Zn_4Cu_3$ and MgZnCu compositional analogs that were coated in a bath from which ferricyanide was withheld. Considering the Raman spectra from these analogs presented in Fig. 2 and 3, clearly, the absence of ferricyanide from the coating bath does nothing to improve CCC formation on the analogs with high levels of Cu.

Based on Raman characterization of CCC formation from ferricyanide baths on Al-Cu-Mg intermetallic compound analogs, McGovern et al. found that CCC formation was suppressed as Cu content of the analog increased.[23] Results showed that CCC formation was suppressed by ferricyanide that strongly adsorbed on the Cu-rich surface. This adsorbed layer retarded CCC formation on the phase, but did not impart corrosion resistance. Results also showed that replacing ferricyanide with an alternate accelerating agent restored CCC formation on the Cu-rich analogs.

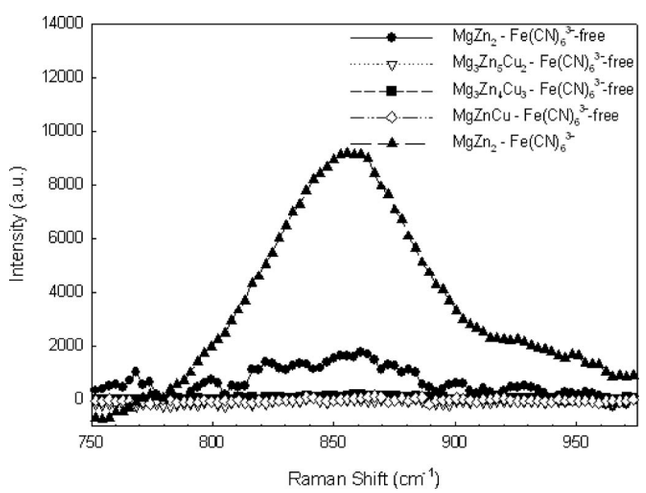

Figure 4. Raman spectra of 3-min CCCs on $MgZn_2$, $Mg_3Zn_5Cu_2$, $Mg_3Zn_4Cu_3$, and MgZnCu coated in a ferricyanide-free bath (Cr + F), and of a 3-min CCC on $MgZn_2$ coated in a ferricyanide-containing bath (Cr + F + Fe).

The Raman results in Fig. 4 indicating the lack of coating formation when ferricyanide is withheld suggest the possibility of another effect in coating formation on η-phase analogs. Several authors have suggested that the passivation of Cu-bearing intermetallic compounds is caused by reductive adsorption of chromate and not by the cyanide adsorption. Halada et al. observed that F and CN ions were not found on Cu-containing compounds after short coating formation times.[24] Hurley and McCreery observed monolayer of chromium(III) film on Cu surface, which was very stable and inhibited electron transfer and further chromate reduction.[25] Campestrini et al. suggested that chromate reduction is intense on Cu-rich intermetallic compounds (IMCs), which leads to rapid CCC formation that prevents adsorption of ferricyanide on IMCs.[26] Which, if any, of these interpretations applies to CCC formation on Cu-bearing η-phase, and why Mg-Zn-Cu intermetallic compounds respond differently than Al-Cu-Mg compounds to conversion coating remains to be determined.

Conclusions

Electrochemical characterization and chromate conversion coating formation experiments with analogs of η-phase with various amounts of dissolved Cu suggest the following

1. Cu dissolved in η over the range of 0–35 atom %, passivates and ennobles the phase.[17]
2. Cu in η tends to suppress the formation of CCCs from ferricyanide-bearing accelerated and ferricyanide-free CCC baths. When the phase contains more than 25 atom % Cu evidence of CCC formation is completely absent in Raman spectra.
3. Ferricyanide accelerates conversion coating formation on $MgZn_2$ just as it does on pure aluminum.
4. Withholding ferricyanide from a coating bath does not restore conversion coating formation on Cu-bearing η suggesting that adsorption of ferricyanide is not responsible for inhibition of CCC formation when the phase contains high concentrations of Cu.

Acknowledgments

This work was supported by the Strategic Environmental Research and Development Program under contract no. DAC72-99-C-0002. The authors appreciate valuable discussions with Dr. T. Ramgopal and Dr. G. S. Frankel.

The Ohio State University assisted in meeting the publication costs of this article.

References

1. L. F. Mondolfo, *Metall. Rev.*, **15**, 95 (1971).
2. L. F. Mondolfo, *Aluminium Alloys: Structure and Properties*, Butterworths, Boston (1976).
3. H. Schmalzried and V. Gerold, *Z. Metallkd.*, **49**, 291 (1958).
4. L. F. Mondolfo, N. A. Gjostein, and D. W. Levinson, *Trans. Am. Inst. Min., Metall. Pet. Eng.*, **206**, 1378 (1956).
5. G. Thomas and J. Nutting, *J. Inst. Met.*, **88**, 81 (1959-1960).
6. R. B. Nicholson, G. Thomas, and J. Nutting, *Br. J. Appl. Phys.*, **9**, 25 (1958).
7. R. B. Nicholson, G. Thomas, and J. Nutting, *J. Inst. Met.*, **87**, 429 (1958-1959).
8. J. Gjonnes and C. J. Simensen, *Acta Metall.*, **18**, 881 (1970).
9. J. D. Embury and R. B. Nicholson, *Acta Metall.*, **13**, 403 (1965).
10. G. W. Lorimer and R. B. Nicholson, *Acta Metall.*, **14**, 1009 (1966).
11. G. W. Lorimer and R. B. Nicholson, *The Mechanism of Phase Transformations in Crystalline Solids*, Inst. Metals, London (1968).
12. J. E. Hatch, *Aluminum Properties and Physical Metallurgy*, American Society for Metals, Metals Park, OH (1984).
13. S. Maitra and G. C. English, *Metall. Trans. A*, **12**, 535 (1981).
14. S. Maitra and G. C. English, *Metall. Trans. A*, **13**, 161 (1982).
15. T. Ramgopal, Ph.D. Thesis, The Ohio State University, Columbus, OH (2001).
16. Q. Meng and G. S. Frankel, *J. Electrochem. Soc.*, **151**, B271 (2004).
17. T. Ramgopal, P. Schmutz, and G. S. Frankel, *J. Electrochem. Soc.*, **148**, B348 (2001).
18. J. K. Park and A. J. Ardell, *Acta Metall. Mater.*, **39**, 591 (1991).
19. Y. Yoon, Ph.D. Thesis, The Ohio State University, Columbus, OH (2004).
20. *Materials Safety Data Sheet for Alodine 1200S*, Henkel Corporation.
21. L. Xia and R. L. McCreery, *J. Electrochem. Soc.*, **146**, 3696 (1999).
22. W. Zhang, B. L. Hurley, and R. G. Buchheit, *J. Electrochem. Soc.*, **149**, B357 (2002).
23. W. R. McGovern, P. Schmutz, R. G. Buchheit, and R. L. McCreery, *J. Electrochem.*

Soc., **147**, 4494 (2000).
24. G. P. Halada, C. R. Clayton, M. J. Vasquez, J. R. Kearns, M. W. Kendig, S. L. Jeanjaquet, G. G. Peterson, G. Shea-McCarthy, and G. L. Carr. in *Critical Factors in Localized Corrosion III, A Symposium in Honor of the 70th Birthday of Jerome Kruger*, R. G. Kelly, G. S. Frankel, P M. Natishan, and R. C. Newman, Editors, PV 98-17, p. 139, The Electrochemical Society Proceedings Series, Pennington, NJ (1999).
25. B. L. Hurley and R. L. McCreery, *J. Electrochem. Soc.*, **150**, B367 (2003).
26. P. Campestrini, H. Terryn, J. Vereecken, and J. H. W. de Wit, *J. Electrochem. Soc.*, **151**, B359 (2004).